

phys. stat. sol. (a) **182**, 709 (2000)

Subject classification: 66.30.Ny; 76.30.Pk; S5

Diffusion and Intercalation of Nitric Acid into Highly Oriented Pyrolytic Graphite: An in situ Conduction ESR Study

A. M. ZIATDINOV, V. V. KAINARA, and A. N. KRIVOSHEI

*Institute of Chemistry, Far Eastern Branch of the Russian Academy of Sciences,
159 Prospekt 100-letiya, 690022 Vladivostok, Russia*

(Received February 11, 2000; in revised form July 3, 2000)

Results of an in situ conduction ESR (CESR) study of HNO_3 molecule intercalation into narrow highly oriented pyrolytic graphite (HOPG) slabs are presented. The changes in the graphite CESR signal line shape, intensity and linewidth and the step-wise changes both of intensity and linewidth of the CESR signal from the intercalated sample have been clearly detected during this reaction. Under the assumption that the graphite CESR signal evolution is caused by the advance of a boundary separating the intercalated and non-intercalated HOPG, the constant of two-dimensional diffusion of nitric acid molecules into HOPG and the average value of the spin reorientation probability during the collision of current carriers with this interface have been extracted from the experimental data.

1. Introduction

In spite of numerous publications devoted to studies of various aspects of graphite intercalation compounds (GICs) structure and properties [1–3], many aspects of the mechanism of “guest” molecule intercalation into graphite have not received sufficient attention. The Conduction ESR (CESR) technique is one of the most powerful methods for studying the graphite intercalation process, because shapes and intensities of the CESR signal both from non-intercalated and intercalated regions of graphite plate vary strongly during the intercalation. However, because of the difficulty of such experiments only a few CESR studies of the graphite intercalation process have been undertaken [4–9]. But even in these cases, because of the presence of the skin effect, the interpretation of changes in the graphite CESR signal during the intercalation process is difficult. This paper is devoted to the results of an in situ CESR study of HNO_3 molecule intercalation into narrow highly oriented pyrolytic graphite (HOPG) slabs (with width being comparable with the skin-depth δ_c governed by the graphite \mathbf{c} -axis conductivity σ_c). The results of a theoretical analysis of the reasons for an increase of graphite CESR signal linewidth during intercalation are also presented.

2. Experimental

CESR measurements were carried out at room temperature using an X-band E-line spectrometer. The constant magnetic field (\mathbf{H}_0) modulation frequency and amplitude

¹) Corresponding author; Tel.: (4232) 311655, Fax: (4232) 311889, e-mail: chemi@online.ru

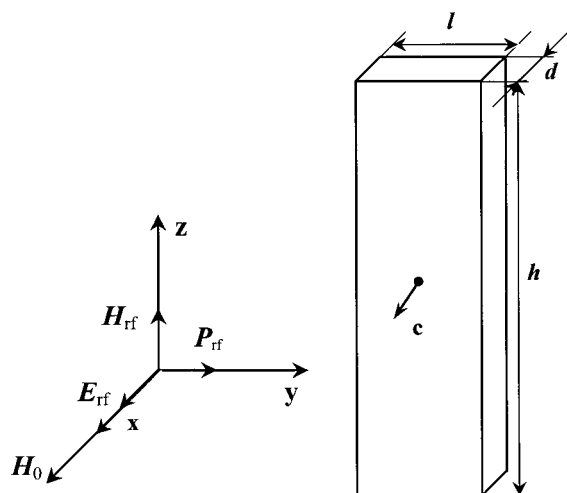


Fig. 1. The orientation of the HOPG plate with respect to the external magnetic field \mathbf{H}_0 and the cavity axis. \mathbf{H}_{rf} , \mathbf{E}_{rf} and \mathbf{P}_{rf} are the magnetic and electric components of the radio-frequency field, and the Poynting vector in an unloaded rectangular cavity, respectively

were 2.5 kHz and 0.1 mT, respectively. The experiments were carried out on HOPG plates with height (h) \times width (l) \times thickness (d) = $0.4 \times 0.04 \times 0.02$ cm³, where $h \times l$ are the dimensions of the basal plane. The HOPG samples were held in a quartz tube connected via a valve to the reservoir with the intercalate (liquid HNO₃ with density $\rho \approx 1.565$ g/cm³). Nitric acid vapours penetrated into the knee of the reactor with the graphite sample through a hole with size $\approx 8 \times 10^{-3}$ cm² in the fluoroplastic diaphragm. Prior to the experiment, the system was evacuated to eliminate air and water. During the measurements, \mathbf{H}_0 was applied along the graphite \mathbf{c} -axis. The basal $l \times h$ and lateral $d \times h$ sides were parallel to the magnetic component (\mathbf{H}_{rf}) of the microwave field (Fig. 1). Note, that in the rectangular resonator, the structure of the electromagnetic field of TE₁₀₂ mode has such a form that, at a conventional setting of the resonator, \mathbf{H}_0 is parallel to the electrical component (\mathbf{E}_{rf}) of microwave field (Fig. 1).

According to data of the four-probe method, at 300 K the σ_c conductivity of the HOPG plate used is equal to $(7.7 \pm 0.8) \Omega^{-1}\text{cm}^{-1}$. In the X-band experiment the value $\delta_c \approx l/2$ corresponds to this conductivity, i.e. the whole volume of the HOPG plate investigated was available for the CESR studies.

3. Results

The CESR spectrum of HOPG plate consists of a single asymmetric line determined by the Dyson mechanism [10]. The spectrum is axial with respect to the \mathbf{c} -axis and is characterized by $g_{\parallel} = 2.0474 \pm 0.0002$ and $g_{\perp} = 2.0029 \pm 0.0002$. The line asymmetry parameter, A/B , being determined as the maximum-to-minimum peak height ratio, both measured with respect to the base line of the first derivative of CESR absorption line, is 'normal' in the sense that the maximum peak height occurs at the lower magnetic fields and it is equal to ≈ 1.8 . For the HOPG samples with $l \gg \delta_c$ the value of A/B is equal to ≈ 4 , i.e. it is essentially 'metallic'. The small value of A/B for the HOPG plate in our experiment is caused by the fact that the CESR lineshape tends to a Lorentzian with $A/B = 1$ at $l \rightarrow 0$.

Several minutes after the injection of the HNO₃ gas into the part of the reactor with the HOPG plate, the CESR signal of graphite begins to transform and decrease in

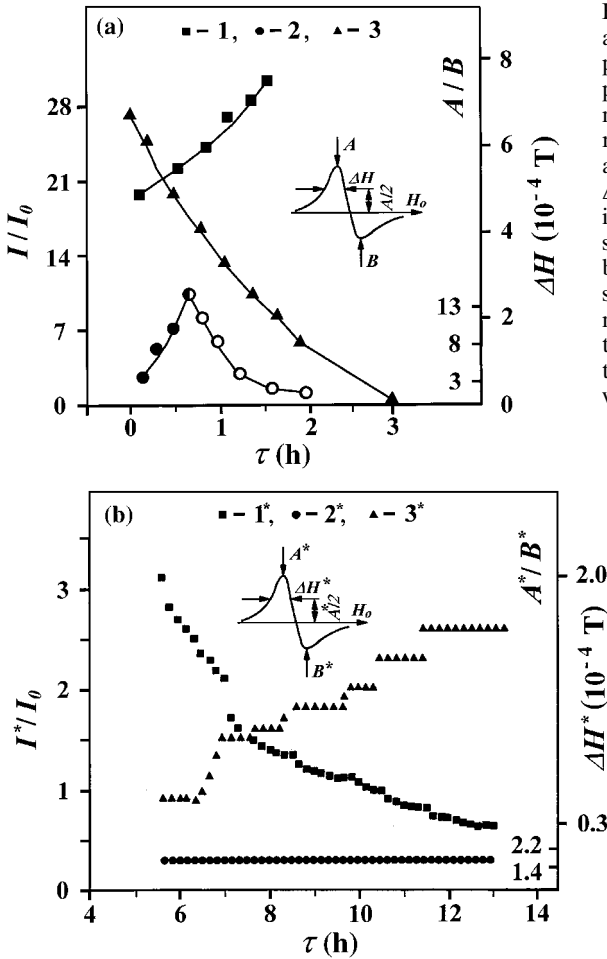


Fig. 2. CESR lineshape parameters for a) non-intercalated and b) intercalated parts of the narrow ($l \approx 2\delta_c$) HOPG plate vs. exposure time, τ , in HNO_3 atmosphere. 1(1*), 2(2*) and 3(3*) correspond to ΔH (ΔH^*), A/B (A^*/B^*) and I/I_0 (I^*/I_0), respectively. $I = (A + B) \Delta H^2$ and $I^* = (A^* + B^*) \Delta H^{*2}$; I_0 is the intensity of the Mn^{2+} ESR signal of the standard sample ($\text{ZnS}:\text{Mn}^{2+}$); the X-band is considered; $T = 300$ K. In a) the shaded and open dots refer to the normal and 'reversed' lineshape, respectively; the half-shaded dot corresponds to the lineshape with symmetric phase with respect to the A peak

intensity until it fully disappears after ≈ 3 h (Fig. 2a). Simultaneously a new signal with $g_{\parallel}^* = 2.0019 \pm 0.0002$ and $g_{\perp}^* = 2.0030 \pm 0.0002$ appears in the spectrum (Fig. 2b), where g_i^* ($i = \parallel, \perp$) is determined by the H_0 value at the point of intersection of the first derivative of the CESR absorption line and the base line.

The linewidth (the intensity), ΔH ($I = (A + B) \Delta H^2$), of the graphite CESR signal increases (decreases) vs. exposure time, τ , monotonously (Fig. 2a). The A/B ratio of the signal increases initially, but it is still 'normal' reaching a maximum value of $A/B \approx 11$. Later, upon further exposure in the intercalate atmosphere, the A/B ratio becomes 'reversed' (the maximum peak height, A, occurs at higher magnetic fields than the peak B), and its magnitude decreases down to ≈ 2 ; the A/B maximum corresponds to the moment when the 'reversal' of the CESR lineshape takes place (Fig. 2a). The g_i ($i = \parallel, \perp$) values of the graphite CESR signal do not change up to its disappearance.

At the beginning of the reaction the linewidth ΔH^* (the peak-to-peak intensity) of the CESR signal with g_i^* is very large (small), and, as a consequence, a large scattering of the CESR signal integral intensity, $I^* = (A^* + B^*) \Delta H^{*2}$, is observed. As τ increases

more than 6 h, this scattering decreases (as a consequence of ΔH^* reduction) and both the $I^*(\tau)$ and $\Delta H^*(\tau)$ dependences take a well-marked step-wise form (Fig. 2b). The asymmetry ratio, A^*/B^* , and g_i^* values of the signal remain constant up to the end of the reaction.

4. Discussion

With the configuration of our ESR experiment (Fig. 1) the microwave field penetrates into the HOPG plate mainly through its lateral sides, which are parallel to both the **c**-axis and **H**_{rf} [11], i.e. through the lateral sides $h \times d$. Therefore, the evolution of the graphite CESR signal of the sample investigated (Fig. 2a) is mainly due to variations of the composition and properties of the HOPG plate at the surface areas from these sides. The dependence of the shape and intensity of the graphite CESR signal on the exposure time of the sample in HNO₃ vapours is qualitatively identical to that of the ESR signal lineshape and intensity of the localized spins in a metallic substrate on the thickness of a spray-coated film of another metal [12]. In our case, the spins in consideration are certainly mobile, but for $l/\delta_c < 2$ the CESR line shape does not depend on the spin mobility [13, 14], i.e., in the framework of the Dyson theory [10] in the HOPG plate investigated the spin carriers may be considered as localized. Therefore, the variations of the shape and intensity of the graphite CESR signal (Fig. 2a) may be considered as being due to the formation of a macroscopic ‘intercalation’ layer on the HOPG plate (with conductivity being different from that of the initial material) and by advance of the interface separating this layer from as-yet the non-intercalated parts of the sample (due to the diffusion of nitric acid molecules into the substrate along the graphite galleries). The invariability of the *g*-factor values for the CESR signal from the HOPG substrate (g_i) and that from ‘intercalation’ layer (g_i^*) up to the disappearance of the signal and the end of reaction, respectively, indicates that the interface between ‘intercalation’ layer and as-yet the non-intercalated parts of sample may be considered as non-conductive. The non-conductivity of this interface may be caused by a significant distortion of the carbon net near the intercalation front and/or by the presence of a high phase-boundary electrostatic potential due to the different current carrier concentration in the intercalated parts of graphite and in the non-intercalated ones.

In the experiment under consideration, the whole volume of the sample investigated is available for CESR studies. Therefore, the time of the graphite CESR signal disappearance corresponds approximately to the moment of contact of the counter (anti-parallel) intercalation fronts. Let us assume that the intercalation is determined by a two-dimensional diffusion-controlled process, i.e. the thickness of the intercalated layer, d^* , depends on the exposure time as $(d^*)^2 = 2D_{\text{int}}\tau$, where D_{int} is the intercalate two-dimensional diffusion constant. In such a case, having substituted the value of time interval from the beginning of the graphite CESR signal transformation up to its disappearance, $\tau \approx 3$ h, and $d^* = l/2$ to this expression, it is easy to estimate the value $D_{\text{int}} \approx 1.8 \times 10^{-12} \text{ m}^2\text{s}^{-1}$. It is worth noting that this value of D_{int} well correlates with that obtained by high-resolution neutron scattering by Simon et al. [15]: $D_{\text{int}} \approx 4 \times 10^{-12} \text{ m}^2\text{s}^{-1}$.

A new and unexpected result of this experiment is the significant broadening of the graphite CESR signal from the beginning of the intercalation up to the contact of the counter intercalation fronts (Fig. 2a). We suppose that the reason for it is the collisions

of current carriers (at their diffusion along the graphite layers) with the non-conductive interface between the intercalated and the non-intercalated parts of the HOPG plate. Indeed, when the intercalation front advances into the HOPG plate (due to the diffusion of nitric acid molecules into the graphite along the galleries) the width of its non-intercalated part decreases and, therefore, the frequency of collisions of graphite current carriers with these interfaces increases. Therefore, assuming the probability of spin reorientation of graphite current carriers during such collisions to be non-zero, the increase of the total rate of spin relaxation of graphite current carriers (the graphite CESR linewidth) with the time of intercalation can be observed. Note, that in all previous ESR experiments on graphite intercalation [4–9] which were carried out on HOPG plates with $l \gg \delta_c$, no broadening of the graphite CESR signal was observed. This indirectly supports our interpretation of the graphite CESR signal broadening at the intercalation of the narrow ($l \approx 2\delta_c$) HOPG plate. (The widening of the CESR signal from the intercalated graphite at lowering of temperature [16–18] and at the disorder–order (liquid–solid) transformation of the HNO_3 layer near 250 K [16–18] is of different nature and, therefore, is not discussed in this paper.)

Using the relation $(d^*)^2 = 2D_{\text{int}}\tau$ the experimental dependence $\Delta H(\tau)$ (Fig. 2a) can be easily transformed into the dependence $\Delta H(a)$, where $a = l - 2d^*$ is the thickness of the non-intercalated part of the HOPG plate (Fig. 3). The latter dependence can be calculated theoretically as well, using the Dyson theory for the CESR in metals, including the effects of surface relaxation [10]. It is assumed in this theory that an electron colliding with the surface has a certain probability ε of spin reorientation, in addition to the steady probability $1/T_2$ (T_2 is the spin-relaxation time due to the collisions of current carriers with the imperfections in the sample volume) which exists for all electrons. In the general Dyson expressions for the CESR line shape [10] the contribution of the surface spin relaxation effects to the CESR line shape is determined by the value of the term $Q = 1/2 G\theta$, where $G = 3\varepsilon/4\lambda$ (λ is the mean free path of current carriers) and θ is the sample thickness. (The analysis of the mentioned Dyson expression has shown that at a given sample thickness the CESR linewidth increases with the parameter G value. For $G \neq 0$, the value of the CESR linewidth tends to infinity at $\theta \rightarrow 0$). Ob-

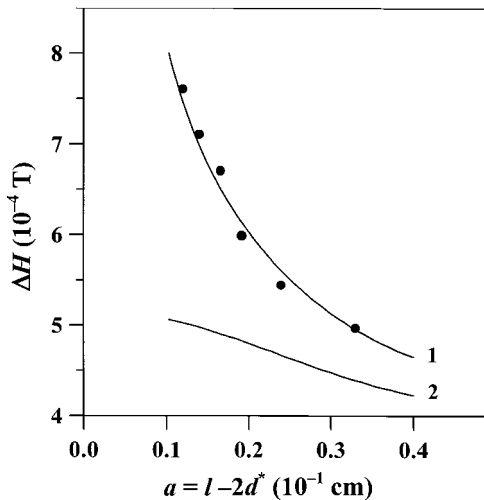


Fig. 3. Graphite CESR linewidth, ΔH , vs. thickness of the non-intercalated part of the HOPG plate: $a = l - 2d^*$. The dots correspond to the experimental data. The lines 1 and 2 correspond to the theoretical graphite CESR linewidth calculated using the Dyson expression [10] with $G = 10$ and 0 cm^{-1} , respectively. The values of $R_a = 2.4$, $\delta_c = 2.6 \times 10^{-2}$ cm and $T_2 = 1.4 \times 10^{-8}$ s for the HOPG plate intercalated, which are necessary for the calculation of these theoretical dependences, were taken from [19]

viously, if ε is considered as an average value of the probability of spin reorientation during collisions of graphite current carriers with the non-conductive phase boundary, then the mentioned expressions can be used for the analysis of the $\Delta H(a)$ dependence also. It is shown in Fig. 3, where the results of such analysis are presented, that the theoretical dependence of the graphite CESR linewidth, with $G = 10 \text{ cm}^{-1}$ describes the experimental data well. (The HOPG values of $T_2 = 1.4 \times 10^{-8} \text{ s}$, T_{Da} (the spin diffusion time for diffusion along the graphite basal plane across the skin-depth δ_c) = $8 \times 10^{-8} \text{ s}$ and $\delta_c = 2.6 \times 10^{-2} \text{ cm}$, which are necessary for the calculation of this dependence were taken from [19].) The found value of G and the typical HOPG values of $A = (0.4\text{--}1.6) \times 10^{-5} \text{ cm}$ [20] correspond to $\varepsilon = (0.5\text{--}2.1) \times 10^{-4}$. It is worth noticing that at present there are no data on interface spin relaxation in conductors in the literature. There are only some published data on surface spin relaxation in simple metals. For comparison, the surface spin reorientation probabilities of conduction electrons in Cu and Li bulk samples are equal to $\sim 10^{-2}$ [21] and $\sim 5 \times 10^{-6}$ [22], respectively.

Experimental data (Fig. 2b) show that the intercalation process is not a continuous one, i.e. it has clear step-wise shape: relatively short time intervals with sharp increase in I^* followed by time intervals with I^* being nearly constant. This fact is in good agreement with known literature data [1, 23–29] reporting that in many cases the graphite intercalation proceeds through the formation of definite intercalation stages and that the amount of intercalate inside the sample and, as a result, the current carrier concentration, increases when the GIC stage index decreases. According to our X-ray diffraction data, the first (last) ‘plateau’ in the experimental dependence $I^*(\tau)$ (Fig. 2b) corresponds to the seventh (second) intercalation stage. Therefore, the number of steps in the $I^*(\tau)$ dependence is equal to the number of possible intercalation stages and the step-wise increase in I^* may be attributed to the sequence of stage transitions from the stages with large integer indices to the stages with small ones.

The presence of two close steps instead of one, corresponding to the sixth stage (Fig. 2b), may be related with the change in the stacking of graphite layers situated between the nearest intercalate layers (stacking transformation). First, such a stacking transformation was observed in the second stage alkali-metal-intercalated graphite by X-ray scattering measurements [30]. In $\text{C}_{5n}\text{HNO}_3$ the stacking transformations were not investigated, but the difference in the stacking sequence in samples with even and odd stage indices was experimentally proved [31–33]. The energy barrier associated with large-scale sliding of carbon layers at the stacking transformation, and corresponding changes in the electronic structure decrease when the stage index decreases. The absence of doubling the number of steps corresponding to the stages with index $n < 6$ in the experiment considered (Fig. 2b) may be explained by this reason.

Since the CESR intensity in metals is proportional to the electron-state density on the Fermi surface, under the above mentioned understanding of the reason for the step-wise dependence of $I^*(\tau)$, the time intervals with invariable value of I^* correspond to the periods during which the insertion of intercalate from the gas phase into the GIC plate is negligible. At this time, the concentration of current carriers in carbon layers does not change, but the reorganization of the intercalate subsystem continues. In particular, this is confirmed by the CESR linewidth decrease within the $I^*(\tau)$ ‘plateau’ (Fig. 2b). The reorganization of the intercalate subsystem during the considered time intervals may consist of splitting and merging of intercalate islands, at simultaneous increase of their mean size, and in agreement with other necessary conditions for

the next stage transition. The time intervals during which the I^* increases (the steps) are determined by the time of advance of the stage changing front into sample on the distance $\approx l/2$. At this time the intercalate layer density increases and charge transfer between intercalate and graphite subsystems takes place. Such scenario of intercalation of narrow HOPG plates (with $l \approx 2\delta_c$) is in agreement with the data of in situ Raman scattering measurements during stage transformations in GICs with HNO_3 [27] and H_2SO_4 [28].

Acknowledgements The authors are grateful to N. M. Mishchenko, V. V. Sereda for help in experiments and to L.B. Nepomnyashchii (Scientific Research Centre for Graphite, Moscow) for providing the HOPG. This work was supported by the Russian Foundation for Basic Research (grant No. 00-03-32610).

References

- [1] M. S. DRESSELHAUS and G. DRESSELHAUS, *Adv. Phys.* **30**, 139 (1981).
- [2] S. A. SOLIN and H. ZABEL, *Adv. Phys.* **37**, 87 (1988).
- [3] P. LAGRANGE, A. HEROLD, and C. HEROLD, *Mol. Cryst. Liq. Cryst.* **310**, 33 (1998).
- [4] R. DAVIDOV, O. MILO, I. PALCHAN, and H. SELIG, *Synth. Met.* **8**, 83 (1983).
- [5] I. PALCHAN, D. DAVIDOV, V. ZEVIN, G. POLATSEK, and H. SELIG, *Phys. Rev. B* **32**, 5554 (1985).
- [6] I. PALCHAN, F. MUSTACHI, D. DAVIDOV, and H. SELIG, *Synth. Met.* **10**, 101 (1984/85).
- [7] M. NAKAJIMA, K. KAWAMURA, and T. TSUZUKU, *J. Phys. Soc. Jpn.* **57**, 1572 (1988).
- [8] A. M. ZIATDINOV, A. K. TSVETNIKOV, N. M. MISHCHENKO, and V. V. SEREDA, *Mater. Sci. Forum* **91/93**, 583 (1992).
- [9] A. M. ZIATDINOV, and N. M. MISHCHENKO, *J. Phys. Chem. Solids* **58**, 1167 (1997).
- [10] F. J. DYSON, *Phys. Rev.* **98**, 349 (1955).
- [11] A. M. ZIATDINOV, and N. M. MISHCHENKO, *Phys. Solid State* **36**, 1289 (1994).
- [12] V. ZEVIN, and J. T. SUSS, *Phys. Rev. B* **34**, 7260 (1986).
- [13] H. KODERA, *J. Phys. Soc. Jpn.* **28**, 89 (1970).
- [14] M. SAINT-JEAN, and E. McRAE, *Phys. Rev. B* **43**, 3969 (1991).
- [15] C. SIMON, I. ROSEMAN, F. BATALLAN, J. ROGERIE, J. F. LEGRAND, A. MAGERL, C. LARTIQUE, and H. FUZELLIER, *Phys. Rev. B* **41**, 2390 (1990).
- [16] S. K. KHANNA, E.R. FALARDEAU, A. J. HEEGER, and J. E. FISCHER, *Solid State Commun.* **25**, 1059 (1978).
- [17] P. LAUGINIE, H. ESTRADÉ, J. CONARD, D. GUERARD, P. LAGRANGE, and M. EL MAKRINI, *Physica* **99B**, 514 (1980).
- [18] A. M. ZIATDINOV, and N. M. MISHCHENKO, *Solid State Commun.* **97**, 1085 (1996).
- [19] A. M. ZIATDINOV, V. V. KAINARA, and A. N. KRIVOSHEI, *Mol. Cryst. Liq. Cryst.* **340**, 307 (2000).
- [20] I. L. SPAIN, in: *Chemistry and Physics of Carbon*, Eds. P. L. WALKER, Jr. and P. A. THROWEER, Marcel Dekker, New York 1973 (Vol. 8, p. 119).
- [21] M. B. WALKER, *Phys. Rev. B* **3**, 30 (1971).
- [22] V. A. ZHIKAREV, A. P. KESSEL, E. G. HARAHASHYAN, F. G. CHERKASOV, and K. K. SHVARZ, *Soviet Phys. - JETP* **64**, 1356 (1973).
- [23] D. E. NIXON and G. S. PARRY, *J. Phys. D* **1**, 291 (1968).
- [24] E. R. FALARDEAU, L. R. HANLON, and T. E. THOMPSON, *Inorg. Chem.* **17**, 301 (1978).
- [25] R. NISHITANI, Y. UNO, and H. SUEMATSU, *Synth. Met.* **7**, 13 (1983).
- [26] M. E. MISENHEIMER and H. ZABEL, *Phys. Rev. Lett.* **54**, 2521 (1985).
- [27] R. NISHITANI, Y. NISHINA, S. HASHIMOTO, and H. IWASAKI, *Synth. Met.* **12**, 161 (1985).
- [28] R. NISHITANI, Y. SASAKI, and Y. NISHINA, *J. Phys. Soc. Jpn.* **56**, 1051 (1987).
- [29] S. A. SAFRAN, *Solid State Phys.* **40**, 183 (1987).
- [30] M. J. WINOKUR, and R. CLARKE, *Phys. Rev. Lett.* **56**, 2072 (1986).
- [31] D. E. NIXON, G. S. PARRY, and A. R. UBBELOHDE, *Proc. Roy. Soc. (London)* **291A**, 324 (1966).
- [32] G. S. PARRY, *Mater. Sci. Engng.* **31**, 99 (1977).
- [33] H. SHAKED, H. PINTO, and M. MELAMUD, *Phys. Rev. B* **35**, 838 (1987).

